

# Polarized Diffuse Emission at 2.3 GHz in a High Galactic Latitude Area

E. Carretti<sup>1\*</sup>, D. McConnell<sup>2</sup>, N. M. McClure-Griffiths<sup>2</sup>, G. Bernardi<sup>1</sup>,  
S. Cortiglioni<sup>1</sup> and S. Poppi<sup>3</sup>

<sup>1</sup>*INAF-IASF Bologna, Via Gobetti 101, Bologna, I-40129, Italy*

<sup>2</sup>*CSIRO-ATNF, P.O. Box 76, Epping, NSW 1710, Australia*

<sup>3</sup>*INAF-IRA Bologna, Via Gobetti 101, Bologna, I-40129, Italy*

Accepted xx xx xx. Received yy yy yy; in original form zz zz zz

## ABSTRACT

Polarized diffuse emission observations at 2.3 GHz in a high Galactic latitude area are presented. The  $2^\circ \times 2^\circ$  field, centred in ( $\alpha = 5^{\text{h}}$ ,  $\delta = -49^\circ$ ), is located in the region observed by the BOOMERanG experiment. Our observations has been carried out with the Parkes Radio telescope and represent the highest frequency detection done to date in low emission areas. Because of a weaker Faraday rotation action, the high frequency allows an estimate of the Galactic synchrotron contamination of the Cosmic Microwave Background Polarization (CMBP) that is more reliable than that done at 1.4 GHz. We find that the angular power spectra of the  $E$ - and  $B$ -modes have slopes of  $\beta_E = -1.46 \pm 0.14$  and  $\beta_B = -1.87 \pm 0.22$ , indicating a flattening with respect to 1.4 GHz. Extrapolated up to 32 GHz, the  $E$ -mode spectrum is about 3 orders of magnitude lower than that of the CMBP, allowing a clean detection even at this frequency. The best improvement concerns the  $B$ -mode, for which our single-dish observations provide the first estimate of the contamination on angular scales close to the CMBP peak (about 2 degrees). We find that the CMBP  $B$ -mode should be stronger than synchrotron contamination at 90 GHz for models with  $T/S > 0.01$ . This low level could move down to 60–70 GHz the optimal window for CMBP measures.

**Key words:** cosmology: cosmic microwave background – polarization – radio continuum: ISM – diffuse radiation – radiation mechanisms: non-thermal.

## 1 INTRODUCTION

The Cosmic Microwave Background Polarization (CMBP) is a powerful tool for investigating the early Universe. For instance, inflationary models lead to a well defined peak-pattern of the  $E$ -mode power spectrum and its precise measurement provides a check of the inflationary paradigm itself (Kosowsky 1999).

The second and fainter CMBP component – the  $B$ -mode – is predicted to directly probe Inflation. In fact, the emission on a few degrees scale is related to the amount of gravitational waves (GW) generated by the Inflation, and allows measurement of its main parameters, such as the energy density of the Universe when this event occurred (Kamionkowski & Kosowsky 1998). On subdegree scales, instead, the  $B$ -mode is contaminated by the  $E$ -mode via galaxy gravitational lensing, allowing though a way to determine the matter fluctuation power spec-

trum (Zaldarriaga & Seljak 1998). The first steps into  $E$ -mode measurements has begun with the detections of the DASI, CAPMAP and CBI experiments (Leitch et al. 2004; Barkats et al. 2004; Readhead et al. 2004). However, we are far from a complete characterization and the  $B$ -mode is still elusive.

Several astrophysical sources of polarized emission in the foreground must be considered as they could contaminate the tiny CMBP signal. Among them, the diffuse synchrotron emission of the Galaxy dominates at low frequencies and it is expected to be the major contaminant up to 100 GHz. Recently, evidence for a significant anomalous dust emission, competitive with the synchrotron up to 50 GHz, has been found (e.g. de Oliveira-Costa et al. 2004; Finkbeiner, Langston & Minter 2004). Although potentially relevant in total intensity, the small polarization fraction predicted (Lazarian & Draine 2000) seems to leave synchrotron as the leading polarized component.

The study of the synchrotron emission is thus crucial for CMBP experiments. Besides the estimate of the contam-

\* E-mail: carretti@bo.iasf.cnr.it

ination level, it allows the tuning of foreground separation procedures to extract the cosmic signal (e.g. Tegmark et al. 2000) and the selection of optimal sky areas for observation.

Polarization measurements with large sky coverage has become available at frequencies up to 1.4 GHz (e.g. see Carretti et al. 2005 and references therein for a review of the available data), although their sensitivities and angular resolutions do not fully cover the CMBP needs. An ideal field for CMBP studies is the high Galactic latitude field ( $b \sim -38^\circ$ ) in the region observed by the BOOMERanG experiment. This field, positioned at  $\alpha = 5^{\text{h}}$ ,  $\delta = -49^\circ$ , has low levels of synchrotron emission and has been selected as the target area for CMBP experiments (e.g. BaR-SPOrt, Cortiglioni et al. 2003, and BOOMERanG-B2K, Masi et al. 2002). The first measurement of the polarized synchrotron emission in low-emission areas was reported by Bernardi et al. (2003) in this field at 1.4 GHz with the Australia Telescope Compact Array (ATCA). The analysis of these observations has allowed the first estimate of the synchrotron contamination on the CMBP spectra at high latitude (Carretti et al. 2005). However, these authors found that at 1.4 GHz the area is likely to be affected by Faraday Rotation (FR) effects, which could enhance the detected emission and modify the spectra by steepening their slopes. In particular, their analysis shows that, at 1.4 GHz this area is in an intermediate state between negligible and significant FR effects. Since FR has a square dependence on the wavelength ( $\delta\varphi \propto \lambda^2$ ), higher frequencies should allow observations of the region without significant effects. Finally, the 1.4 GHz data have an angular scale sensitivity range limited by the interferometric nature of the observations, and cover only the angular scales up to 15 arcmin.

To overcome these constraints, we have conducted single dish observations of this area at 2.3 GHz with the Parkes Radio telescope. These observations also allow us to extend the angular scale sensitivity toward degree scales, leading to a firmer assessment of the contamination of the CMBP  $B$ -mode generated by GW, which peaks on  $\sim 2^\circ$  scales.

The paper is organized as follows: in Section 2 we present details of the observations along with the discussion of the obtained maps. In Section 3 we show the analysis of the angular power spectra, while in Section 4 we discuss the implications for CMBP measurements.

## 2 OBSERVATIONS

We have made single dish observations of the  $2^\circ \times 2^\circ$  area centred in  $\alpha = 5^{\text{h}}00^{\text{m}}00^{\text{s}}$ ,  $\delta = -49^\circ00'00''$  (J2000) ( $l \sim 255^\circ$ ,  $b \sim -38^\circ$ ) with the Parkes Radio telescope at 2.3 GHz on 17–23 August 2004. The field was surveyed with  $2^\circ$  scans in both RA and Dec. Scans were separated by 3 arcmin, providing an adequate sampling of the  $8'8$  telescope beam. We used the dual circular polarization Galileo receiver in combination with a wide band 13 cm feed. The two total intensity channels and the two linear Stokes parameters,  $Q$  and  $U$ , were formed from the auto and cross correlations of the two receiver outputs. The digital correlator was configured to provide 1024 250 kHz-channels, giving a total bandwidth of 256 MHz centered on 2300 MHz. In the subsequent analysis the channels have been grouped in  $8 \times 32$  MHz. The system showed an optimal sensitivity in a

200 MHz wide band. After the selection for RF interferences, a total effective bandwidth of  $\Delta\nu = 128$  MHz has remained with a central frequency of 2332 MHz.

The sources 1934-638 and 3C138 have been used for total intensity and polarization calibration, respectively. The absolute polarization state of 3C138 was determined using ATCA one week prior to the Parkes observations. Although 3C138 is variable, the timescale is such that the one week lag between observations is insignificant (Padielli et al. 1987).

Images of the Stokes parameters  $I$ ,  $Q$  and  $U$  were constructed through an iterative map-making procedure, based on the estimation and removal of a linear baseline from each scan. The image produced at each iteration is used in the next to subtract the sky signal from the data and improves the baseline evaluation (see Sbarra et al. 2003 for the basic equations and Carretti & Poppi, in preparation, for an implementation at the Medicina Radio telescope). Differing from Sbarra et al. (2003), a linear behaviour for the baseline is allowed. As usual, the removal of a linear baseline leads to the loss of the absolute emission levels in the images.

The Stokes  $I$ ,  $Q$ ,  $U$  and linearly polarized intensity,  $L = \sqrt{Q^2 + U^2}$ , images are shown in Figure 1. The images cover an area of  $2^\circ \times 2^\circ$ , have a pixel size of 3 arcmin, and have an rms pixel sensitivity of  $1.0 \text{ mJy beam}^{-1}$  or  $800 \mu\text{K}$  in brightness temperature units (the gain is  $0.77 \text{ Jy/K}$ ). Finally, they have been smoothed to a FWHM of  $10'.6$ .

The total intensity emission is dominated by point sources, corresponding to the strongest sources in the 1.4 GHz image (Carretti et al. 2005). The polarization images are dominated by diffuse emission. Structures are present on all angular scales up to the field size, with the largest feature extending from north to south. Excluding the one evident point source, the polarized intensity image peaks at about 5 mK, while the peak-to-peak variation of  $U$  is of about 10 mK ( $Q$  shows less power).

The small range of overlapping angular scales in the 1.4 and 2.3 GHz observations makes a direct comparison difficult. However, it is worth noting the filamentary structure about 1 degree long present at 1.4 GHz has no counterpart at 2.3 GHz but approximately corresponds with the maximum gradient of the 2.3 GHz  $U$  map. It is possible that this structure is generated by a Faraday screen at 1.4 GHz, as supposed also by Bernardi et al. (2003), but the structure disappears at 2.3 GHz, where FR is weaker.

An image of the polarization angle is shown in Figure 2. The pattern is uniform inside the large structures but sudden changes of about  $90^\circ$  are observed when crossing a zero in polarized intensity. These features can have physical origins, such as the effects of a Faraday screen or a sudden change in the magnetic field direction. However, here they correspond to a change of sign of  $U$  (the dominant component) and are characterized by a  $\sim 90^\circ$  change of polarization angle. This could be simply generated by a mean value removal. The addition of a constant value to  $U$  would eliminate this change of sign, keeping more uniform the polarization angle pattern. Map-making procedures can generate such a situation, therefore, besides the presence of either a Faraday screen or a rapid change of the magnetic field, the sudden changes in polarization angle of our map can be related to this non-physical cause. Only observations of a larger area can provide the missing mean emission and distinguish the two cases.

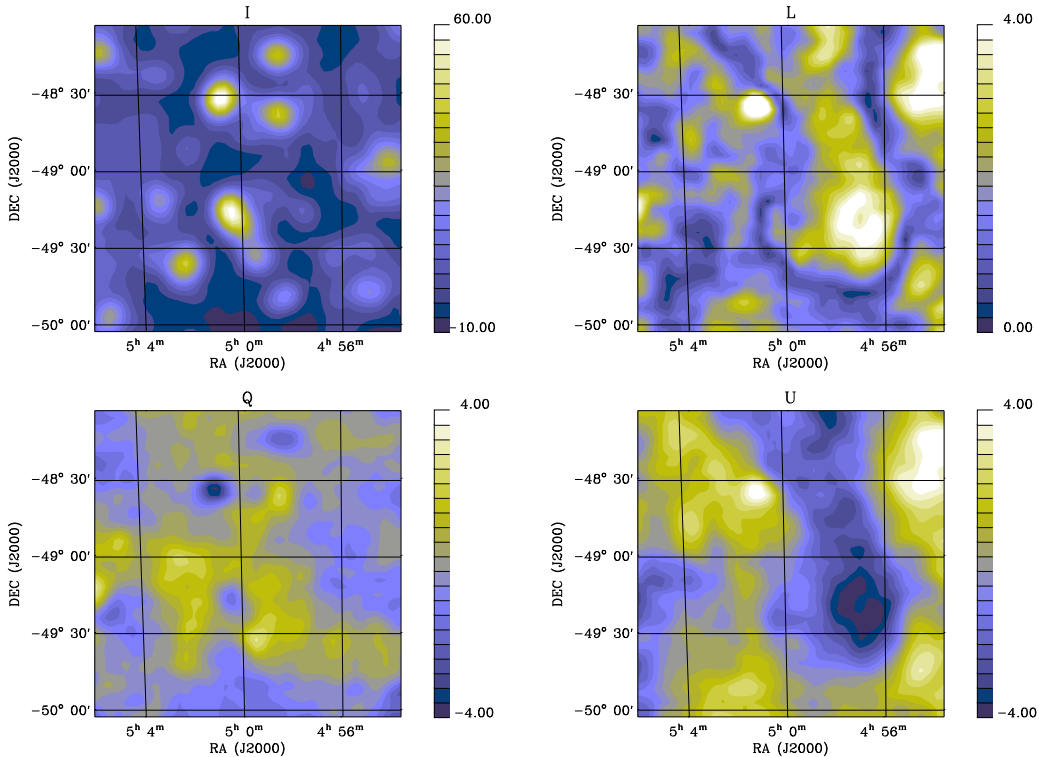


**Figure 1.** Maps of the Stokes parameters  $I$  (top-left),  $Q$  (bottom-left) and  $U$  (bottom-right) of the observed area at 2.3 GHz. The polarized intensity  $L = \sqrt{Q^2 + U^2}$  is shown as well (top-right). Units are mK.

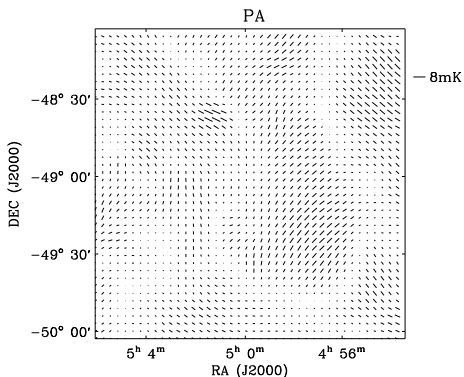


**Figure 2.** Polarization angle map. The vector length is proportional to the polarized intensity.

### 3 POWER SPECTRUM ANALYSIS

We compute the power spectrum of the  $E$ - and  $B$ -modes of the polarized component through the Fourier technique of Seljak (1997). The results are shown in Figure 3 together with power law fits to the equation:

$$C_\ell^X = C_{500}^X \left( \frac{\ell}{500} \right)^{\beta_X}, \text{ with } X = E, B, \quad (1)$$

where  $\ell$  is the multipole, corresponding to the angular scale  $\theta \approx 180^\circ/\ell$ . The spectra of  $E$ - and  $B$ -mode have similar power, except at smaller  $\ell$ , where the poor statistics allows larger deviations between the two components. The results of the fits are given in Table 1.

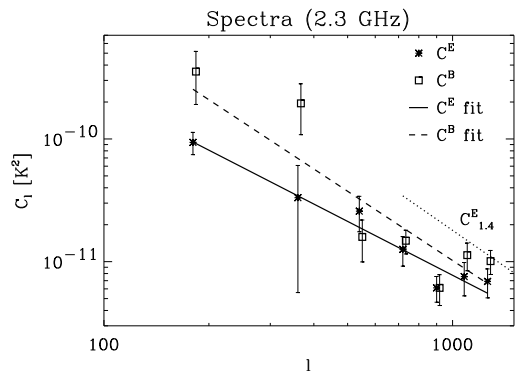


**Figure 3.** Angular power spectra  $C_\ell^E$  and  $C_\ell^B$  in the observed area together with their power law fits.  $C_\ell^B$  is slightly shifted to the right to avoid confusion. The fit to the 1.4 GHz  $E$ -mode power spectrum scaled up to 2.332 GHz ( $C_{1.4}^E$ ) is also displayed (a frequency spectral slope of  $\alpha = -2.8$  is assumed).

**Table 1.** Fit parameters for  $E$  and  $B$  spectra.

Spectrum	$C_{500}^X [10^{-12} \text{ K}^2]$	$\beta_X$
$C_\ell^E$	$21 \pm 2$	$-1.46 \pm 0.14$
$C_\ell^B$	$37 \pm 6$	$-1.87 \pm 0.22$

The comparison with the spectra obtained in the same area at 1.4 GHz (Carretti et al. 2005) allows interesting considerations. Figure 3 plots the 1.4 GHz spectrum scaled to

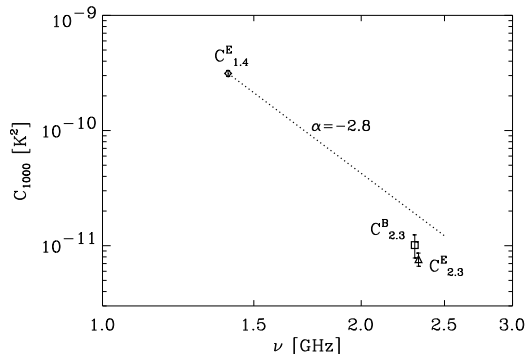


**Figure 4.** Fits to power spectra  $C_\ell^X$  computed at  $\ell = 1000$  for both 1.4 GHz and 2.3 GHz.  $E$ - and  $B$ -mode are almost overlapped at 1.4 GHz, so that the latter has been omitted to avoid confusion. Similarly,  $C_{2.3}^B$  is slightly shifted left to avoid confusion. The dotted line represents the 1.4 GHz value extrapolated using a brightness temperature slope of  $\alpha = -2.8$ .

2.3 GHz with a brightness temperature frequency spectral slope  $\alpha = -2.8$ , while Figure 4 shows the  $E$ -mode powers for  $\ell = 1000$  at 1.4 and 2.3 GHz. The  $E$ -mode emission level of our 2.3 GHz observations is significantly weaker than expected for a synchrotron spectrum with slope of  $\alpha = -2.8$ . In fact, a frequency spectral index of  $\tilde{\alpha}_E = -3.6 \pm 0.15$  is required to fit the amplitudes. A similar view is given by the  $B$ -mode, although the needed slope is flatter ( $\tilde{\alpha}_B = -3.3 \pm 0.2$ ). Such steep slopes are unlikely at these frequencies for synchrotron emission (Platania et al. 1998). We suggest that the amplitudes at 1.4 GHz are affected by FR. This suggestion is supported by Carretti et al. (2005), who find that randomization of polarization angles induced by FR can transfer power from large to small angular scales, enhancing the power on subdegree scales. At 2.3 GHz, where Faraday effects are less than at 1.4 GHz, the observed polarization is more closely related to the intrinsic emission, as discussed in Carretti et al. (2005). Thus it seems clear that observations at higher frequencies are more robust for CMB extrapolation.

The comparison between the slopes of the angular power spectra provides a similar view. At 2.3 GHz  $\beta_E$  is flatter than at 1.4 GHz, where a value of  $\beta_E^{1.4} \sim -1.97 \pm 0.08$  has been measured. The values measured at 2.3 GHz are closer to the mean value  $\beta_X^{GP} \sim -1.6$  ( $X = E, B$ ) obtained on the Galactic plane at the same frequency (Bruscoli et al. 2002). Carretti et al. (2005) discussed the effects of the FR on the power spectrum slope, finding that steepening can occur if FR action is significant. In this context, the flatter slope measured at 2.3 GHz can be interpreted as FR effects being weak relative to those at 1.4 GHz. We note that the  $B$ -mode cannot be fit well with a power law (see Figure 3), so that the resulting larger error makes  $\beta_B$  compatible with both  $\beta_B^{1.4} = -1.98 \pm 0.07$  and  $\beta_X^{GP}$ . Therefore, no firm statements can be made about the comparison of  $\beta_B^{1.4}$  and  $\beta_B$ .

#### 4 DISCUSSION

The steep spectral index needed to match the 1.4 GHz emission level, the regularity in the polarization angle pattern,

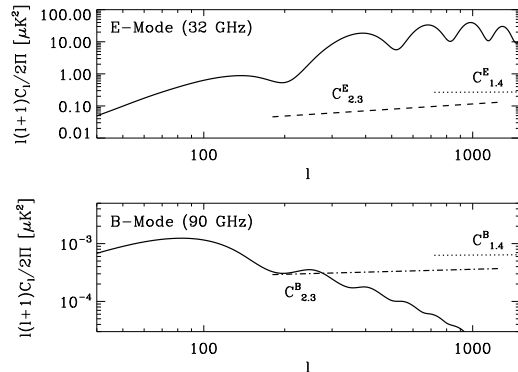


**Figure 5.** Angular power spectra  $C_\ell^E$  (top) and  $C_\ell^B$  (bottom) extrapolated to 32 GHz and 90 GHz, respectively, of both the 2.3 and 1.4 GHz data. A frequency spectral slope of  $\alpha = -3.1$  is assumed. Spectra expected for the CMBP are shown for comparison (solid) by using cosmological parameters determined with the WMAP data (Spergel et al. 2003). For the  $B$ -mode, a tensor-to-scalar power ratio  $T/S = 0.01$  is assumed.

and the flatter slope of the 2.3 GHz  $E$ -mode angular power spectrum, indicate that our maps are weakly affected by FR effects. Consequently, they provide the most reliable estimates of the contamination of the CMBP by synchrotron emission at high Galactic latitudes. Moreover, these data explore larger angular scales than possible with the 1.4 GHz observations (limited to scales smaller than  $15'$ ), allowing estimates closer to the peak of the  $B$ -mode emission at about  $2^\circ$  ( $\ell \sim 100$ ).

The extrapolations up to 32 GHz ( $E$ -mode) and 90 GHz ( $B$ -mode) are shown in Figure 5, where the typical spectral index  $\alpha = -3.1$  of the 1.4–2.3 GHz range has been assumed (Bernardi et al. 2004). The contamination of the  $E$ -mode is significantly lower than that estimated with the 1.4 GHz data: a factor two better is seen at  $\ell \sim 1000$ , while the flatter slope of the 2.3 GHz angular spectrum increases that factor at larger scales to about 4 at  $\ell = 400$ . Note that the  $\ell$ -range now covered allows a direct estimate on angular scales usually probed by 30 GHz experiments (e.g. the 32 GHz channel of BaR-SPOrt with a FWHM =  $0.4^\circ$ ). This improves the expected detectability of the CMBP  $E$ -mode signal, by avoiding the uncertainties of an angular extrapolation. At 32 GHz, the first CMBP peak ( $\ell \sim 400$ ) is about 3 orders of magnitude above the synchrotron emission (i.e. a factor 30 in signal). This makes us confident that in this area the cosmic signal is detectable by experiments in this band. Even considering an uncertainty of  $\Delta\alpha = 0.2$  in the spectral index (Platania et al. 1998; Bennett et al. 2003), the extrapolation would change by a factor  $\sim 3$  in spectrum, not significantly affecting the previous conclusion. In addition, our estimate strengthens the results obtained by the CMBP experiments, which find indications that at 30 GHz the emission of this foreground is not dominant (Leitch et al. 2004; Readhead et al. 2004). At 90 GHz the frame is even better: the synchrotron  $E$ -mode is 5 orders of magnitude weaker than the CMB, giving a very negligible contamination in the CMB frequency window.

Our measurements allow even larger improvements in the expected detectability of the  $B$ -mode component. The improved coverage of the angular spectrum gives a more

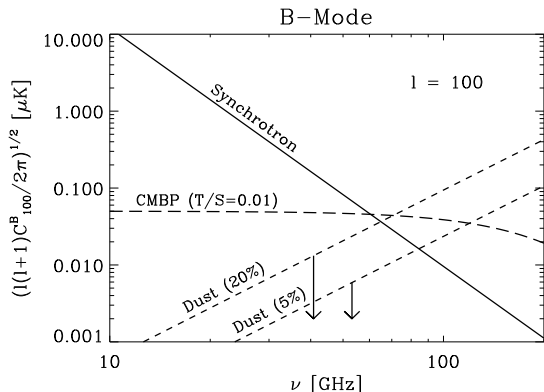


**Figure 6.** Frequency behaviour of the synchrotron and dust  $B$ -mode in our patch. The quantity  $\sqrt{\ell(\ell+1)C_\ell^B/(2\pi)}$  in  $\ell = 100$  is shown because a fair estimate of the signal on the scale where the CMB  $B$ -mode peaks ( $\theta \sim 2^\circ$ ). The CMB level expected in the case of  $T/S = 0.01$  is plotted for comparison. Synchrotron emission is estimated by extrapolating to  $\ell = 100$  the fit of Table 1. We assume a slope of  $\alpha = -3.1$  for the frequency behaviour. Dust emission is evaluated from the total intensity upper limit measured with the BOOMERanG experiment at  $b = -38^\circ$  (Masi et al. 2001). A slope of  $\alpha = 2.2$  is assumed for the frequency extrapolation (Bennett et al. 2003). Two values of polarization fraction (5% and 20%) are used to bracket the 10% deduced by Benoît et al. (2004) for high Galactic latitudes.

reliable estimate of the  $B$ -mode contamination near the  $\ell \sim 100$  CMBP peak. The power of this peak is expected to vary with the tensor-to-scalar perturbation ratio  $T/S$  so measuring the level of the GW background in the early Universe. Our data suggest that at 90 GHz the synchrotron contamination dominates the CMBP signal for models with  $T/S < 0.01$ , allowing the detection of this still unknown parameter well below its present upper limit ( $T/S < 0.90 - 95\%$  C.L.: Spergel et al. 2003).

The resulting picture is encouraging: in this area of the sky the CMBP  $E$ -mode is expected a factor 30 larger than the synchrotron emission at  $\sim 30$  GHz, so appearing free of this contaminant, even allowing for possible uncertainties in the frequency extrapolation. At 90 GHz the contamination on the  $E$ -mode is negligible, while that on the  $B$ -mode appears to dominate the CMB signal only for models with  $T/S < 0.01$ . This low level is beyond the capability of the the PLANCK mission ( $\Delta(T/S) \sim 0.06 - 95\%$  C.L.: see Tegmark et al. 2000) and only future experiments devoted to the search of the  $B$ -mode will be limited by the foreground emission in this sky area.

Although an accurate estimate of the dust contribution in the area cannot be done due to the many uncertainties, we indicate some plausible upper limits in Figure 6. These, and our new lower estimate of the synchrotron component, suggest that the thermal dust could become the most important source of foreground noise at 90 GHz. This would move the optimal window for  $B$ -mode investigations from 90–100 GHz toward 70 GHz, as for the CMB anisotropy (Bennett et al. 2003). Better estimates of the optimum  $B$ -mode observing frequency require a direct measure of the polarized dust emission in this sky area, possibly at higher frequency where the dust emission is stronger.

## ACKNOWLEDGMENTS

This work has been carried out in the frame of the SPOrt experiment, a program funded by ASI (Italian Space Agency). G.B. and S.P. acknowledge ASI grants. We wish to thank Bob Sault for the ATCA observations of 3C138, Warwick Wilson for his support in the Wide Band Correlator setup, and John Reynolds for his support in the receiver setup. Part of this work is based on observations taken with the Parkes Radio telescope, which is part of the Australia Telescope, funded by the Commonwealth of Australia for operation as a National Facility managed by CSIRO. We acknowledge the use of the CMBFAST package.

## REFERENCES

- Barkats D., et al., 2004, ApJ, 619, L127  
 Bennett C.L., et al., 2003, ApJS, 148, 97  
 Benoît A., et al., 2004, A&A, 424, 571  
 Bernardi G., Carretti E., Cortiglioni S., Sault R.J., Kesteven M.J., Poppi S., 2003, ApJ, 594, L5  
 Bernardi G., Carretti E., Fabbri R., Sbarra C., Cortiglioni S., Poppi S., Jonas J.L., 2004, MNRAS, 351, 436  
 Bruscoli M., Tucci M., Natale V., Carretti E., Fabbri R., Sbarra C., Cortiglioni S., 2002, New Astron., 7, 171  
 Carretti E., Bernardi G., Sault R.J., Cortiglioni S., Poppi S., 2005, MNRAS, in press, astro-ph/0412598  
 Cortiglioni S., et al., 2003, in Warmbein B., ed., 16th ESA Symposium on European Rocket and Balloon Programmes and Related Research, ESA Proc. SP-530, p. 271  
 de Oliveira-Costa A., Tegmark M., Davies R.D., Gutiérrez C.M., Lasenby A.N., Rebolo R., Watson R.A., 2004, ApJ, 606, L89  
 Finkbeiner D.P., Langston G.I., Minter A.H., 2004, ApJ, 617, 350  
 Kamionkowski M., Kosowsky A., 1998, PRD, 57, 685  
 Kosowsky A., 1999, New Astron. Rev., 43, 157  
 Lazarian A., & Draine B.T., 2000, ApJ, 536, L15  
 Leitch E.M., Kovac J.M., Halverson N.W., Carlstrom J.E., Pryke C., Smith M.W.E., 2004, astro-ph/0409357  
 Masi S., et al., 2001, ApJ, 553, L93  
 Masi S., et al., 2002, in Cecchini S., Cortiglioni S., Sault R.J., Sbarra C., eds, Astrophysical Polarized Backgrounds, AIP Conf. Proc., 609, 122  
 Padrielli L., et al., 1987, A&AS, 67, 63  
 Platania P., Bensadoun M., Bersanelli M., de Amici G., Kogut A., Levin S., Maino D., Smoot G.F., 1998, ApJ, 505, 473  
 Readhead A.C.S., et al., 2004, Science, 306, 836  
 Sbarra C., Carretti E., Cortiglioni S., Zannoni M., Fabbri R., Macculi C., Tucci M., 2003, A&A, 401, 1215  
 Seljak U., 1997, ApJ, 482, 6  
 Spergel D.N., et al., 2003, ApJS, 148, 175  
 Tegmark M., Eisenstein D.J., Hu W., de Oliveira-Costa A., 2000, ApJ, 530, 133  
 Zaldarriaga M., Seljak U., 1998, PRD, 58, 23003